CHEMISTRY
A European Journal

A Journal of
ChemPubSoc Europe

Accepted Article

Title: Insulin-Delivery from Glucose-Responsive Self-Assembled Polyamine Nanoparticles: Smart "Sense-and-Treat" Nanocarriers Made Easy

Authors: Maximiliano Agazzi, Santiago Herrera, M. Lorena Cortez, Waldemar Marmisollé, Mario Tagliazucchi, and Omar Azzaroni

To be cited as: *Chem. Eur. J.* 10.1002/chem.201905075

Link to VoR: http://dx.doi.org/10.1002/chem.201905075

Supported by
ACES

WILEY-VCH

10.1002/chem.201905075

Insulin-Delivery from Glucose-Responsive Self-Assembled Polyamine Nanoparticles: Smart "Sense-and-Treat" Nanocarriers Made Easy

Maximiliano L. Agazzi,[a] Santiago E. Herrera,[a] M. Lorena Cortez,[a] Waldemar A. Marmisollé,[a] Mario Tagliazucchi,[b] Omar Azzaroni*[a]

[a] Instituto de Investigaciones Fisicoquímicas Teóricas y Aplicadas Facultad de Ciencias Exactas, Universidad Nacional de La Plata–CONICET Sucursal 4, Casilla de Correo 16, 1900 La Plata, Argentina.

[b] Departamento de Química Inorgánica, Analítica y Química Física, INQUIMAE-CONICET Facultad de Ciencias Exactas y Naturales, Ciudad Universitaria, Pabellón 2, Buenos Aires C1428EHA, Argentina.

e-mail: azzaroni@inifta.unlp.edu.ar

Abstract

Polyamine-salt aggregates (PSA) are biomimetic soft-materials that have attracted great attention due to their straightforward fabrication methods, high drug-loading efficiencies and attractive properties for pH-triggered release. Here, a simple and fast multicomponent self-assembly process was used to construct crosslinked poly(allylamine hydrochloride)/phosphate PSAs (hydrodynamic diameter of 360 nm) containing glucose oxidase enzyme, as a glucose-responsive element, and human recombinant insulin, as a therapeutic agent for the treatment of diabetes mellitus (GI-PSA). The addition of increasing glucose concentrations promotes the release of insulin due to the disassembly of the GI-PSAs triggered by the catalytic in-situ formation of gluconic acid. While under normoglycemia, the GI-PSA integrity remained intact for at least 24 h, hyperglycemic conditions produced a 100% of cargo releasing after 4 h of glucose addition. This entirely supramolecular strategy presents great potential for the construction of smart glucose-responsive delivery nanocarriers.

Introduction

Rational and nature-inspired engineering of responsive delivery nanoarchitectures emerged as a fascinating challenge in materials science and modern biomedicine.[1–6] Within this context, the development of intelligent glucose-sensitive delivery devices to treat diabetes mellitus has prompted substantial research advances.[7–10] This metabolic disease is characterized by a deficit of endogenously produced insulin and/or insulin resistance that leads to elevated blood glucose levels (hyperglycemia).[11] Currently, diabetes mellitus affects more than 400 million people around the world, being one of the most serious threats to world public health.[12,13] In general, diabetic patients self-administer insulin with multiple subcutaneous injections to control blood glucose levels.[14–16] However, this methodology is usually painful and requires strict compliance on the part of the patient. In addition, open-loop subcutaneous administration of insulin often regulates inadequately the glucose levels, causing very severe disorders.[17–19] Therefore, several investigations have focused on the design of glucose-sensitive delivery systems with capacity to sense glucose levels and use this information to selectively activate the insulin release in hyperglycemia conditions (closed-loop insulin delivery).[18,20–22] Generally, to achieve the selective response, a glucose-responsive material is incorporated into the delivery platform, such as the glucose-oxidase enzyme (GOx).[23,24] GOx catalyzes the oxidation of D-glucose to gluconic acid, which in turn reduces the local pH.[25,26][27] In this way, the acidic pH can lead to conformational or structural changes in the delivery systems that ultimately drive the release of insulin.

Glucose-sensitive materials with entrapped GOx have been increasingly studied employing architectures based on hydrogels, microgels and multilayer films[28–30], in which GOx is immobilized in complex macromolecular systems.[31] The use of tailorable polymeric (nano)particles offers attractive features for drug delivery systems, including suitable colloidal stability, large surface-volume ratios, high loading capacity, long circulation time in plasma and ability to cross biological membranes.[32–36] In this way, several self-regulated insulin delivery systems based on vesicles, micelles and nanogels have been presented.[37–42] Typically, these nanocarriers are formed by self-assembly or crosslinking of sensitive block copolymers. The synthesis of these building blocks requires multi-step processes that increase costs

and hinder the design scalability for practical applications. Therefore, the development of facile and robust engineering approaches to build innovative nanoscale platforms is an exciting challenge.

In parallel, bioinspired polyamine-salt aggregates (PSA) based on the ionic crosslinking of polyamines have been intensively explored in the last decades for delivery of drugs, proteins, genes and medical imaging agents.[43,44] These soft materials have become a focus of attention mainly due to three crucial advantages: (1) their preparation involves a very simple one-step process based on the mixture of dilute polyelectrolyte solutions with multivalent salts under mild conditions;[45,46] (2) their three-dimensional matrices present a great capacity to integrate different types of bioactive and functional compounds;[47–52] (3) they respond to external stimuli, such as pH and ionic strength, because the supramolecular network is essentially stabilized by electrostatic interactions.[53–56] Within this framework, poly (allylamine hydrochloride) (PAH) was used as a building block to generate PSA by crosslinking with simple inorganic phosphate (Pi).[57,58]

In this sense, PAH/Pi PSA have been used to encapsulate functional compounds such as indocyanine green (ICG) and curcumin.[59–61] Moya and co-workers also used a PAH/Pi PSA as a nanocarrier for pH-triggered release of small interfering RNA (siRNA).[62] They found that the PSA loaded with siRNA remains stable at physiological pH, and releases its cargo in acidic endosomes, where the protonation of the phosphate groups destabilize the electrostatic interactions that support the ionically crosslinked matrix. Very recently, we explored the physicochemical properties and the pH/ionic strength response of PAH/Pi PSA in solution phase.[63] We also used PSAs loaded with a model molecular dye as building blocks for the construction of multilayer films with attractive properties for pH-controlled release.[64]

In the present work, we show for the first time the co-immobilization and rational integration of proteins in the crosslinked PAH/Pi PSA. In particular, we pursue the goal of integrating both GOx and insulin into the ionically crosslinked PAH/Pi matrix to obtain a new kind of glucose-responsive soft material. We demonstrated that it is possible to generate the multi-component nanoarchitecture by a

simple preparation process and that the resulting supramolecular nanocarriers present interesting properties for glucose-regulated insulin delivery.

Materials and methods

Chemicals:

Poly(allylamine hydrochloride) (PAH) (M_w~17500), glucose oxidase (GOx) from Aspergillus niger (type VII), insulin human recombinant (Ins) (SAFC, 91077C) and 4-(2-hydroxyethyl)piperazine-1-ethanesulfonic acid (HEPES) were purchased from Sigma Aldrich. Sodium phosphate monobasic monohydrate (Pi) was purchased from Cicarelli. D-(+)-glucose (Glu), sodium hydroxide and hydrochloric acid were purchased from Anedra. All chemicals were used without further purification.

GOx-Insulin-containing polyamine-salt aggregate (GI-PSA) assembly:

In order to obtain 10 mL of a GI-PSA colloidal dispersion, we consecutively mixed the following solutions in a 50 mL beaker under constant stirring (50 rpm): 1) 2.34 mL of PAH (20 mM, monomer concentration), 2) 22.1 mL of HEPES buffer (20 mM, pH=7.4), 3) 1.95 mL of GOx (2 mg mL^{-1}), 4) 1.95 mL of Ins (2 mg mL^{-1}) and 5) 1.731 mL of Pi (10 mM). All solutions (PAH, GOx, Ins, and Pi) were freshly prepared using a 20 mM aqueous solution of HEPES buffer as solvent and their pH values were adjusted to 7.4 using 1 M HCl or 1 M NaOH prior to mixing. We added each solution very quickly into the beaker to avoid heterogeneous reactions and waited 5 min between the addition steps. After the incorporation of Pi, 30 mL of a cloudy solution was obtained (0.13 mg mL^{-1} Ins, 0.13 mg mL^{-1} GOx, 1.56 mM PAH and 0.577 mM Pi). The as-prepared colloidal dispersion was allowed to stabilize for 2 h under stirring to complete the crosslinking process. The dispersion was then centrifuged at 4000 rpm (RCF=1310 g) for 30 min and the supernatant was discarded to remove the excess of reactants (UV-Vis analysis of polypeptide content in the supernatant is shown in the Supporting Information, Figure S1). The precipitate was concentrated three times in 20 mM HEPES buffer (pH=7.4) and re-suspended by

ultrasonication for 15 min to yield 10 mL of GI-PSA colloidal dispersion. The resuspended dispersion was used for pH and glucose-triggered disassembly experiments.

GI-PSA disassembly by external pH changes:

The turbidity of the GI-PSA colloidal dispersion was tested at different pH values by measuring the transmittance percentage (%T) at λ=580 nm (light-scattering effects). To study the disassembly process, 50 mM HCl was added in small aliquots (0.5 - 2 µl) to 2 mL of GI-PSA colloidal dispersion while measuring pH and %T. A clear solution (100 %T) indicated total GI-PSA disassembly.

GI-PSA disassembly by glucose addition:

For glucose-induced disassembly studies, 2 mL of GI-PSA colloidal dispersion was placed in a plastic cuvette and thermostatized at 37 ºC. A small volume of glucose 0.5 M in 20 mM HEPES buffer (pH=7.4) was added into the cuvette and a chronometer was turned on. The solution was gently air-injected every 20 minutes and both the pH and %T at λ=580 nm were registered, keeping the temperature stable at 37 ºC. pH values were registered using a capilar pH-electrode connected to an ADWA AD8000 pH-meter.

Dynamic light scattering (DLS) measurements:

DLS measurements were carried out using a ZetaSizer Nano (ZEN3600, Malvern, U.K.) at 37 °C employing DTS1060 disposable cuvettes. The detector was placed at 173° backscatter angle and all measurements were conducted using 10 runs of 20 s.

Transmission electron microscope (TEM) measurements:

TEM images were obtained using a JEOL microscope (120 kV) equipped with a Gatan US1000 CCD camera. Samples were stained with phosphotungstic acid and adsorbed on carbon grids. The GI-

PSA transference to the grids was achieved by forming a meniscus between the grid (top) and a concentrated GI-PSA colloidal dispersion (bottom) for a few seconds, followed by air-drying.

Circular dichroism (CD) spectroscopy measurements:

CD measurements were performed using a Jasco (Tokyo, Japan) J-815 CD spectrometer at 20 °C. A quartz cuvette with a 1-mm path length was used for the peptide region (200 – 250 nm). Each spectrum is the result of the averaging of 5 consecutive scans. PSA sample contained 0.13 mg mL^{-1} GOx, 1.56 mM PAH and 0.577 mM Pi in 20 mM HEPES buffer at pH=7.4. Free GOx sample contained 0.13 mg mL^{-1} GOx in 20 mM HEPES buffer at pH=7.4.

Transmittance (%T) measurements:

The transmittance of GI-PSA colloidal dispersions was measured using an Ocean Optics DH-2000 at λ=580 nm with 1-cm light-path plastic cuvettes.

UV-Visible spectroscopy measurements:

UV-Visible experiments were carried out using a Perkin Elmer Lambda 35 spectrometer and a 2-mm light-path quartz cuvette.

Results and Discussion

GI-PSA characterization and pH-triggered disassembly:

By a simple combination of the individual building blocks under mild conditions (room temperature, neutral pH, atmospheric pressure, and aqueous solution), we constructed a PAH/Pi polyamine-salt aggregate (PSA) that contains glucose oxidase and human recombinant insulin (GI-PSA) (Scheme 1). At pH=7.4, the negative net charge of these two proteins allows for their integration into the GI-PSA crosslinked structure. As we previously showed, the main phosphate species that contributes to

10.1002/chem.201905075

the PAH/Pi PSA assembly is the HPO_4^{2-} anion, which strongly interacts with the positively charged amine groups in PAH chains [63].

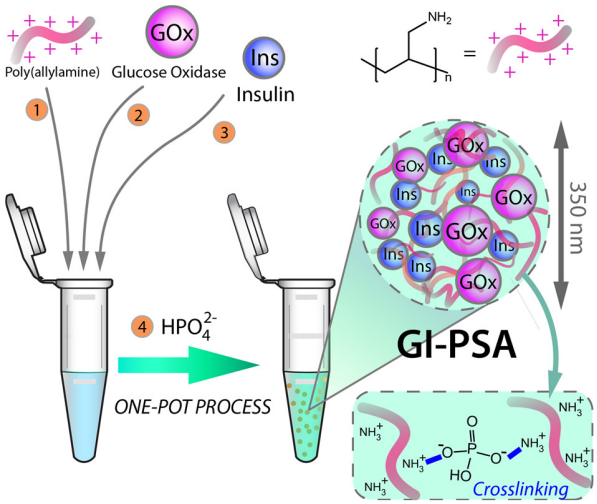

Scheme 1. GI-PSA formation at neutral pH. PAH crosslinking with phosphate anions and co-encapsulation of glucose oxidase (GOx, violet spheres) and insulin (Ins, blue spheres).

Figure 1a shows the size distribution of GI-PSAs obtained from dynamic light-scattering (DLS) measurements at 37 °C (pH=7.4). A single peak centered at 360 nm with a polydispersity index of 0.1 indicates a narrow and homogeneous distribution of sizes in the solution phase. This result is consistent with the hypothesis that the crosslinking of PAH occurs concomitantly with the uptake of insulin and GOx. On the other hand, the TEM image in Figure 1b shows that GI-PSAs have a spherical shape and a wide distribution of particle diameters with a maximum at 90 nm and a tail at large diameter. The fact that TEM sizes are smaller than DLS ones is probably due to dehydration of the sample for TEM measurement. Furthermore, GI-PSAs may suffer partial deformation when in contact with surfaces.[64]

10.1002/chem.201905075

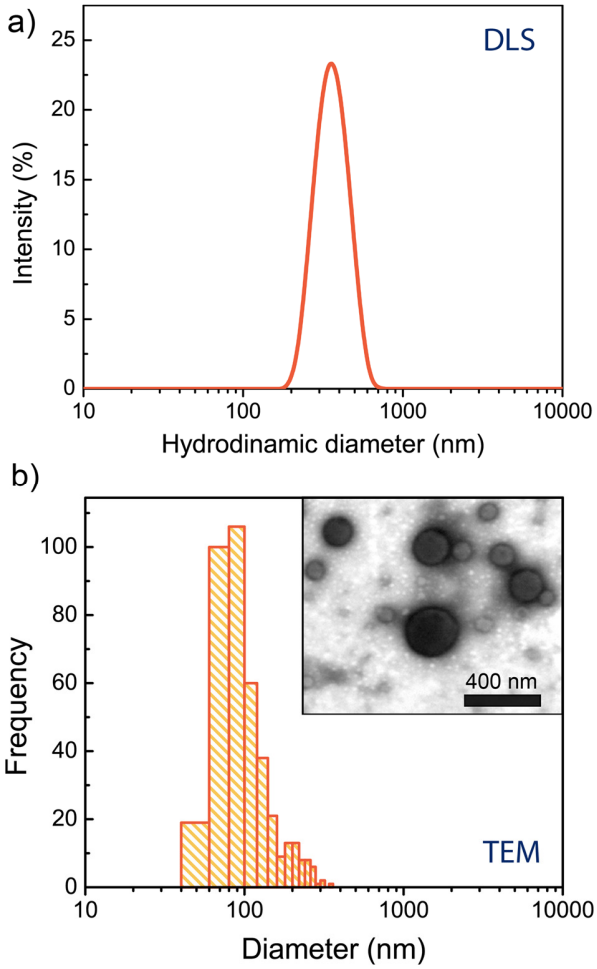

Figure 1. GI-PSA size distribution obtained by DLS (a) and TEM (b) analysis. Inset shows a TEM image of a GI-PSA sample.

We tested the stability of GI-PSAs over time in order to evaluate the possibility of non-selective undesired release of proteins. For this purpose, after 24 h of assembly, the sample was centrifuged, and the supernatant was analyzed by UV-Vis spectroscopy. Both GOx and insulin have absorption bands around 275 nm due to the presence of tryptophan or tyrosine residues.[65,66] In addition, GOx exhibits absorption bands at 375 nm and 450 nm that are characteristic of the flavin adenine dinucleotide cofactor bound to the protein structure.[67] The spectrum of the supernatant showed a much smaller absorption in the UV and visible regions than a solution containing only GOx and Insulin at the same final concentration of the colloidal sample (0.39 mg mL^{-1}). This result indicates that the protein cargo is efficiently encapsulated inside the GI-PSA structure and stabilized by supramolecular interactions and

that undesired protein release does not occurs (Figure S2). This result is not trivial, since it shows that it is possible to rationally integrate two functional proteins in PAH/Pi PSAs through a simple protocol and using only supramolecular interactions. Previously, Anderson and co-workers reported the development of glucose-responsive microgels based on a physically crosslinked matrix of chitosan/tripolyphosphate loaded with insulin.[28] However, in that example, the GOx enzyme had to be first covalently encapsulated in nanocapsules, and then incorporated into the microgels.

The secondary structure of the GOx encapsulated in PSA was studied by CD spectroscopy. Figure S3 shows the far-UV CD spectra of free and encapsulated GOx in HEPES buffer at pH=7.4. The CD spectrum of native GOx exhibited two negative minima in the ultraviolet region around at 207 and 220 nm, which are characteristic of an α-helical conformation.[68–71] GOx within PSA also present a negative shift in the CD signal similar to that observed for the free enzyme, revealing a permanence of the helix conformation. However, the CD band at 207 nm lowers its intensity in a 60%. This could indicate a decrease in the α-helical content and changes in the secondary structure of the enzyme due interactions with polyamine chains.

As we previously reported, a PAH/Pi crosslinked colloid can be disassembled by altering the pH of the solution.[63] At low ionic strength conditions, if the pH is below 5.5, the HPO_4^{2-} anions that act as GI-PSA crosslinker get protonated completely forming the $H_2PO_4^{1-}$ ions. As this monovalent anion is not able to act as a crosslinking agent, the complete dissolution of the GI-PSAs is produced. On the other hand, if the pH is raised above 9.7, the amine groups in PAH get deprotonated and the GI-PSAs also dissolve. This behavior represents one of the key features of GI-PSAs as can be used for pH-triggered release of therapeutic drugs.[43,44,72]

The integrity of GI-PSAs was evaluated as a function of the pH by measuring the light scattering of a GI-PSA colloidal dispersion at different pH values. For this purpose, we measured the transmittance of the sample at λ=580 nm while lowering the pH by adding small aliquots of HCl. Light extinction at this wavelength is exclusively due to scattering, therefore an increase in the transmittance reflects a

10.1002/chem.201905075

decrease of either the number or the mean size of GI-PSA particles. Figure 2a shows the transmittance at λ=580 nm between pH=7.4 and pH=4. A slow increase in the transmittance is detected until pH=5.25 and, after this point, a marked increase is observed reaching 50% of transmittance at pH=5.1, and 100% at pH=4.8. Figure 2b shows two photographs of the sample before and after disassembly. In the latter, a translucent solution indicates quantitative dissolution of GI-PSA colloids by addition of acid. The critical pH required to dissolve the colloids is lower in the present system than in an analog system without insulin and GOx.[63] This extra-stabilization produced by the addition of the proteins can be attributed to the electrostatic coupling between the negatively charged insulin/GOx macromolecules ($pI_{insulin}$=5.3 ; pI_{GOx}=4.2) and the protonated PAH chains.[65,73,74] In other words, the proteins also act as crosslinking agents together with the phosphate anions.

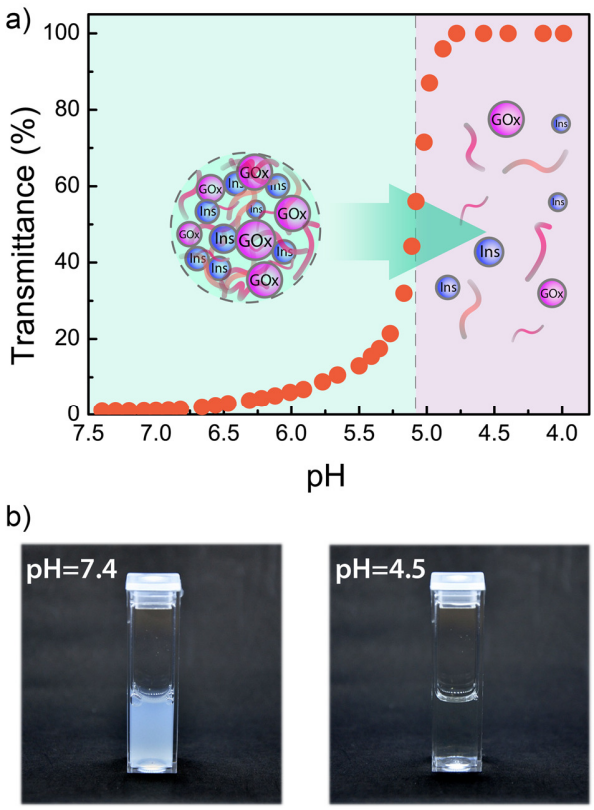

Figure 2. a) Total transmittance at λ=580 nm for a GI-PSA colloidal dispersion vs. pH. The pH was externally adjusted by addition of HCl. b) Photographs of the GI-PSA colloidal dispersion at pH=7.4 (left) and pH=4.75 (right).

Glucose-triggered GI-PSA disassembly:

GOx enzyme catalyzes the oxidation of glucose by dissolved molecular oxygen.[25,75] The products of the reaction are D-glucono-δ-lactone and hydrogen peroxide. In a following reaction step, the D-glucono-δ-lactone hydrolyzes to gluconic acid (pKa=3.86). Thus, at pH values higher than the pKa of gluconic acid, the oxidation of glucose concomitantly releases protons that lower the pH of the solution. In this way, the oxidation of glucose catalyzed by the GOx loaded into the GI-PSA is expected to dissolve the colloids by indirect shifting of the solution pH.

In order to evaluate the glucose responsiveness, GI-PSAs were incubated at 37°C in solutions with different glucose concentrations, including hyperglycemic levels (10, 15 and 20 mM),[76] a normoglycemic level of 5 mM,[77] and a control level of 0 mM. We recorded the time variation of the pH and %T immediately after the addition of glucose (see Figure 3a and 3b, respectively). The results show that the pH drops over time and the rate of pH change increases with increasing glucose level. This behavior reveals that GOx, immobilized in the ionic matrix, preserves its catalytic capabilities. On the other hand, under conditions of normoglycemia (5 mM), the pH reaches a constant value of 6.75 after 4 h, and then it remains stable for more than 2 days (not shown).

10.1002/chem.201905075

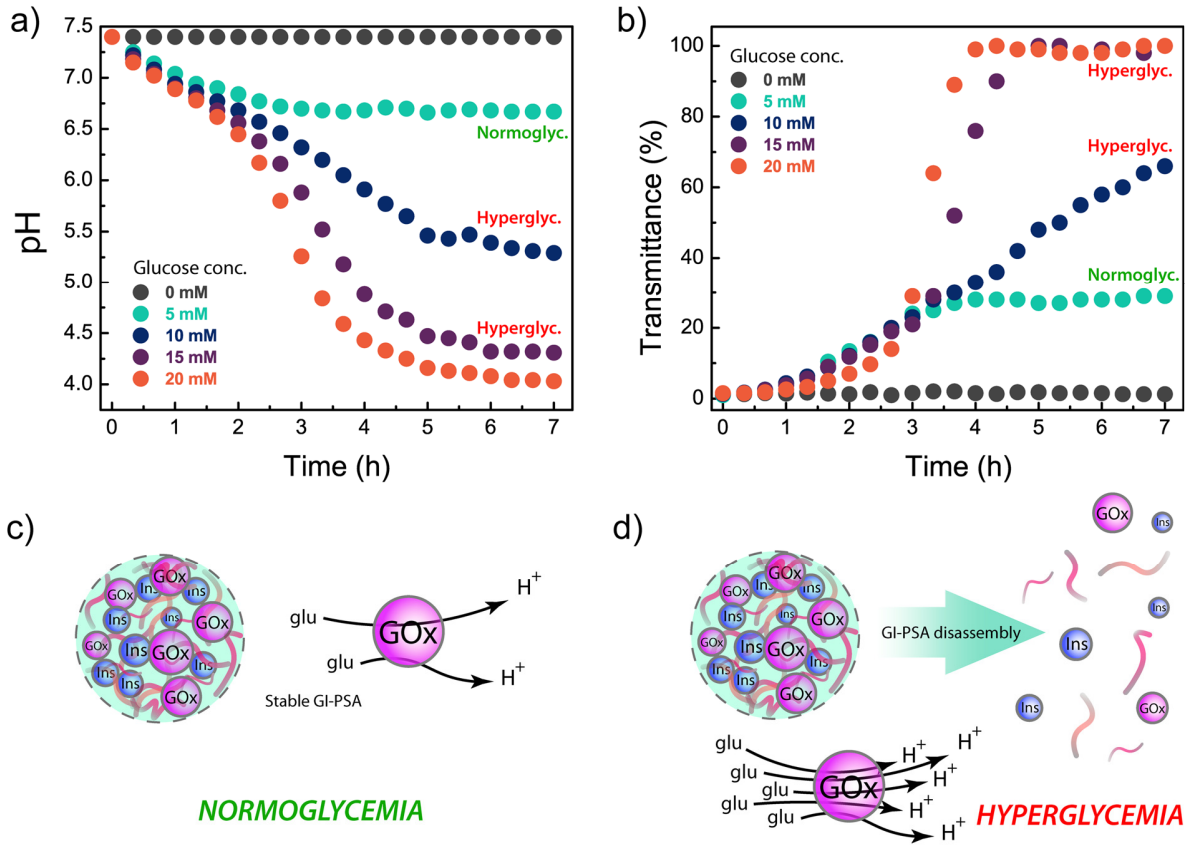

Figure 3. Time evolution of GI-PSAs after addition of 0 mM, 5 mM, 10 mM, 15 mM and 20 mM glucose: (a) pH vs. time (b) transmittance at λ=580 nm vs. time. Simplified representation of GI-PSA stability in normoglycemia (c) and hyperglycemia (d).

The time variation of the sample transmittance (Figure 3b) shows a marked increase for the cases of 20 and 15 mM glucose concentration, reaching %T = 100% after 4 and 5 h, respectively. This result indicates that the total dissolution of GI-PSAs is achieved under hyperglycemic conditions (Figure 3d), releasing the total content of protein into the media. The complex evolution of the pH over time observed in Figure 3a can be numerically simulated considering the acid/base equilibria of the different components in the solution and the typical Michaelis-Menten kinetics of the enzyme. Figure S4 shows that both experimental and theoretical curves follows the same sigmoidal shape, demonstrating that the changes in the solution pH can be explained in terms of a combination between the rate of gluconic acid production by GOx and the different degree of acid and buffer dissociation. A detailed description of the model used for the calculation of the pH changes over time is presented in the electronic supplementary

10.1002/chem.201905075

information. For both 15 and 20 mM samples, the total GI-PSA disassembly is produced when the pH reaches a critical value of 4.5 (Figure 3a), similar to the dissolution pH obtained in the pH-forced disassembly experiment (Figure 2a). This result is consistent with the hypothesis that the dissolution of GI-PSAs is produced by the partial protonation of HPO_4^{2-} and the consequent loss of its crosslinking properties. This result has great significance as it proves that the release of insulin can be indirectly triggered by increasing glucose concentration.

While in the case of 10 mM glucose concentration, a constant increase in the transmittance is detected during 7 h, in conditions of normoglycemia (5 mM) the transmittance linearly increase for the first 3.5 h and finally reaches a stable value of 26% that remains constant over 2 days at 37°C (not shown). After this period of time, the sample (5 mM) was analyzed by DLS obtaining a homogeneous distribution of particle sizes with a maximum centered at a diameter of 400 nm (Figure S5 b), similar to the case of a freshly prepared GI-PSA colloidal suspension (Figure 1a). This observation indicates that, if the pH is high enough (pH=6.75), the GI-PSAs remain stable in solution due to the presence of HPO_4^{2-} anions acting as crosslinking agents (Figure 3c).

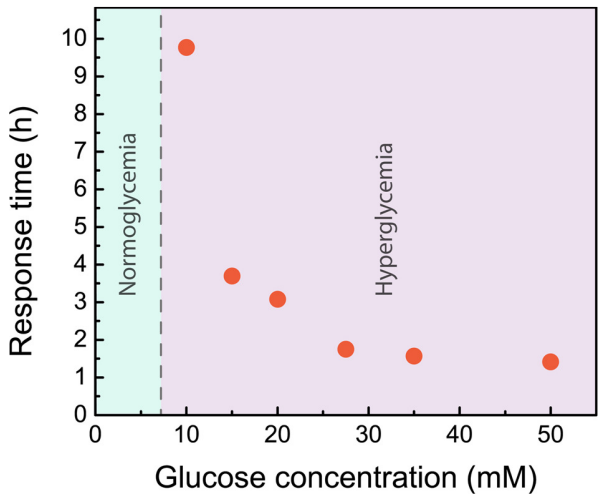

Figure 4. GI-PSA response time (%T (λ=580 nm) = 50%) vs. glucose concentration. GOx saturation effects.

10.1002/chem.201905075

Figure 4 shows the GI-PSA response time (defined as the time at which the colloidal suspension reaches 50% transmittance at λ=580 nm) as a function of the concentration of added glucose. The obtained data indicate that the disassembly kinetics of GI-PSAs can be easily modulated by changing the glucose concentration. Also, the GI-PSA disassembly time decreases considerably as the glucose concentration increases until reaching a constant value around 1.5 h for glucose levels higher than 30 mM. The Michaelis constant for GOx with glucose is around 20 mM,[75] which indicates that the appearance of the plateau in Figure 4 is probably caused by the saturation of the enzyme at high glucose concentration.

Finally, we evaluated the glucose-triggered insulin release. The percentage of total protein (GOx + insulin) released was measured after 48 h of GI-PSA incubation with different concentrations of glucose (Figure 5). For this propose, each GI-PSA colloidal suspension was centrifuged, and the corresponding supernatants were analyzed by UV-Vis spectroscopy (Figure 5a). The total protein content, referred as 100 %, was obtained by analyzing the UV-Vis spectrum at λ=275 nm of a GI-PSA solution after complete disassembly with HCl (pH=4.5).

10.1002/chem.201905075

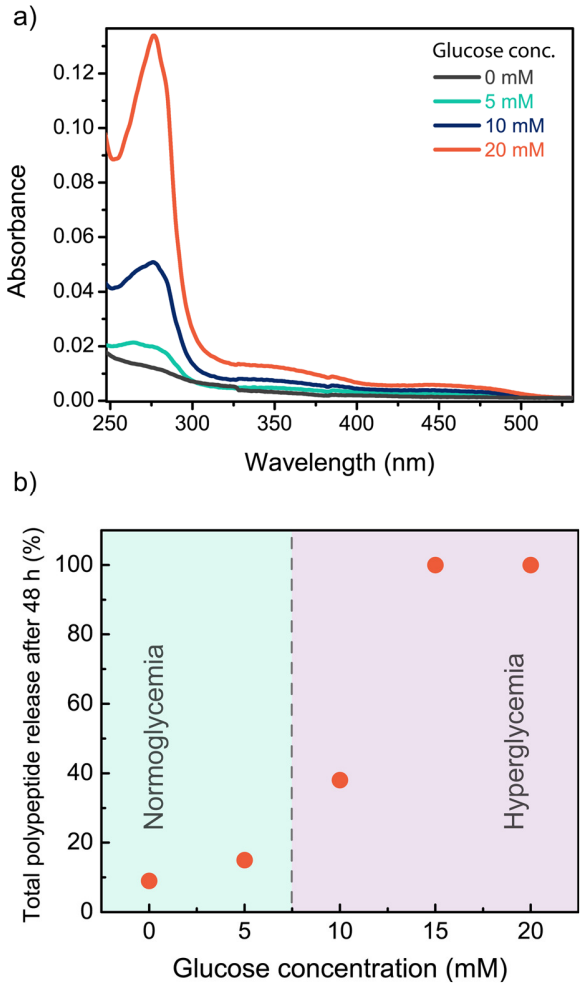

Figure 5. a) UV-visible spectra of centrifuged GI-PSA supernatant 48 h after glucose addition and b) percentage of total protein released (GOx + Insulin) into the solution by spectral analysis at λ=275 nm.

Figure 5b shows that, in the absence of glucose, the release of proteins from GI-PSAs was 9%. This small value indicates that the system has a suitable stability and keeps its cargo trapped after 48 hours of preparation. In normoglycemia conditions (5 mM of glucose), a small release of around 15% of the total trapped protein was found, which is in congruence with the minor changes of pH and transmittance as a function of time observed in Figure 3. In addition, this observation is in line with the homogeneous distribution of the particle sizes found by DLS after 48 h of incubation (Figure S5). When the GI-PSAs were exposed to hyperglycemia conditions, the amount of released protein grew considerably, reaching a 100% for the cases of 15 and 20 mM glucose, in accordance with the complete GI-PSA disassembly observed in Figure 3. When 10 mM glucose was added, a 40% of the total

polypeptide was released, which indicates that the 60% remained linked to the GI-PSA structure after 48 h. The change of the amount of released protein with the glucose concentration indicates that our nanocarrier has the ability to self-regulate the insulin release rate and fraction depending on the concentration of glucose in the media.

Conclusions

In summary, a new insulin delivery approach has been proposed based on the co-immobilization of GOx and insulin into a biomimetic polyamine-salt aggregate. This straightforward engineering route leads to the successful construction of entirely supramolecular spherical nanocarriers by simple mixing the subunits in mild conditions.

The GI-PSA obtained in this work has the capacity to sense glucose levels and respond by activating the release of insulin. Under hyperglycemic conditions, the GOx trapped in the GI-PSA colloids converts glucose to gluconic acid, which results in an acidic environment that triggers the dissociation of the ionic pairs in the supramolecular structure and, consequently, promotes the insulin release. In contrast, negligible insulin release was observed under normoglycemia conditions.

We believe this PSAs-based non-covalent strategy has great potential for the generation of an efficient and robust glucose-responsive insulin delivery system. In order to adjust the system to operate in physiological conditions, further studies must be carried out checking the GI-PSA stability over time under *in vivo* conditions for different glucose levels and GOx contents. The main challenge in the application of glucose-responsive systems is to achieve a rapid response rate in physiological environment with highly regulated pH. In this sense, it is essential that the glucose-responsiveness under hyperglycemia conditions generates a fast change of local pH that overcomes the physiological regulation and activates the selective release of insulin. Although direct comparison with other GOx-based platforms is difficult due to the different experimental conditions used in each case, under *in vitro* conditions other pH-controlled insulin release systems exhibited responses on time scales similar

to that observed for our system.[1–3] Interestingly, some of these systems were explored *in vivo* by subcutaneous administration in 3D-gels-based configurations and showed great ability to regulate blood glucose concentrations.[4–6] Thus, a future challenge for the implementation of PSA as an effective on-demand insulin-releasing agent could be the development of semi-permeable PSA shells that allow significant local pH changes despite the body's natural pH regulation.

Finally, it is worth highlighting that the successful co-immobilization of two biomacromolecules, as GOx and insulin, opens the possibility of exploring the encapsulation and hierarchical combination of other therapeutic and functional agents into the polyamine/phosphate PSAs, as well as the possibility of developing nanoreactors for enzymatic cascade reactions.

Acknowledgements

This work was supported by the Consejo Nacional de Investigaciones Científicas y Técnicas (CONICET, Argentina) (Grant No. PIP 0370), Agencia Nacional de Promoción Científica y Tecnológica (ANPCyT, Argentina; PICT-2016-1680, PICT-2017-1523), the Austrian Institute of Technology GmbH (AIT-CONICET Partner Group: *"Exploratory Research for Advanced Technologies in Supramolecular Materials Science",* Exp. 4947/11, Res. No. 3911, 28-12-2011), and Universidad Nacional de La Plata (UNLP). M.L.C., W.A.M, M.T. and O. A. are staff members of CONICET. M.L.A and S.E.H. gratefully acknowledge CONICET for their postdoctoral fellowships. The authors gratefully acknowledge Dr. Pablo H. Di Chenna for his helpful assistance during CD measurements.

Keywords: Drug delivery • Nanostructures • Supramolecular chemistry • Self-assembly • Molecular recognition

[1] B. Taghizadeh, S. Taranejoo, S. A. Monemian, Z. Salehi Moghaddam, K. Daliri, H. Derakhshankhah, Z. Derakhshani, *Drug Deliv.* **2015**, *22*, 145–155.

[2] M. Karimi, A. Ghasemi, P. Sahandi Zangabad, R. Rahighi, S. M. Moosavi Basri, H. Mirshekari, M. Amiri, Z. Shafaei Pishabad, A. Aslani, M. Bozorgomid, et al., *Chem. Soc. Rev.* **2016**, *45*, 1457–1501.

[3] M. Liu, H. Du, W. Zhang, G. Zhai, *Mater. Sci. Eng. C* **2017**, *71*, 1267–1280.

[4] L. Zhao, Q. Zou, X. Yan, *Bull. Chem. Soc. Jpn.* **2019**, *92*, 70–79.

[5] K. Ariga, D. T. Leong, T. Mori, *Adv. Funct. Mater.* **2018**, *28*, 1702905.

[6] M.-T. Li, M. Liu, Y.-H. Yu, A.-W. Li, H.-B. Sun, *Bull. Chem. Soc. Jpn.* **2019**, *92*, 283–289.

[7] R. Mo, T. Jiang, J. Di, W. Tai, Z. Gu, *Chem. Soc. Rev.* **2014**, *43*, 3595.

[8] N. A. Bakh, A. B. Cortinas, M. A. Weiss, R. S. Langer, D. G. Anderson, Z. Gu, S. Dutta, M. S. Strano, *Nat. Chem.* **2017**, *9*, 937–943.

[9] O. Veiseh, B. C. Tang, K. A. Whitehead, D. G. Anderson, R. Langer, *Nat. Rev. Drug Discov.* **2015**, *14*, 45–57.

[10] J. Yu, Y. Zhang, H. Bomba, Z. Gu, *Bioeng. Transl. Med.* **2016**, *1*, 323–337.

[11] D. R. Owens, B. Zinman, G. B. Bolli, *Lancet* **2001**, *358*, 739–746.

[12] S. Wild, G. Roglic, A. Green, R. Sicree, H. King, *Diabetes Care* **2004**, *27*, 1047–1053.

[13] X. Jin, D. D. Zhu, B. Z. Chen, M. Ashfaq, X. D. Guo, *Adv. Drug Deliv. Rev.* **2018**, *127*, 119–137.

[14] N. Jeandidier, S. Boivin, *Adv. Drug Deliv. Rev.* **1999**, *35*, 179–198.

[15] S. Yaturu, *World J. Diabetes* **2013**, *4*, 1.

[16] R. Shah, M. Patel, D. Maahs, V. Shah, *Int. J. Pharm. Investig.* **2016**, *6*, 1.

[17] Y. Ohkubo, H. Kishikawa, E. Araki, T. Miyata, S. Isami, S. Motoyoshi, Y. Kojima, N. Furuyoshi, M. Shichiri, *Diabetes Res. Clin. Pract.* **1995**, *28*, 103–117.

[18] K. M. Bratlie, R. L. York, M. A. Invernale, R. Langer, D. G. Anderson, *Adv. Healthc. Mater.* **2012**, *1*, 267–284.

[19] D. R. Owens, *Nat. Rev. Drug Discov.* **2002**, *1*, 529–540.

[20] T. G. Farmer, T. F. Edgar, N. A. Peppas, *J. Pharm. Pharmacol.* **2008**, *60*, 1–13.

[21] V. Ravaine, C. Ancla, B. Catargi, *J. Control. Release* **2008**, *132*, 2–11.

[22] Q. Wu, L. Wang, H. Yu, J. Wang, Z. Chen, *Chem. Rev.* **2011**, *111*, 7855–7875.

[23] J. Xie, A. Li, J. Li, *Macromol. Rapid Commun.* **2017**, *38*, 1700413.

[24] L. Zhao, L. Wang, Y. Zhang, S. Xiao, F. Bi, J. Zhao, G. Gai, J. Ding, *Polymers (Basel).* **2017**, *9*, 255.

[25] S. B. Bankar, M. V. Bule, R. S. Singhal, L. Ananthanarayan, *Biotechnol. Adv.* **2009**, *27*, 489–501.

[26] M. J. Webber, D. G. Anderson, *J. Drug Target.* **2015**, *23*, 651–655.

[27] M. L. Cortez, A. Lorenzo, W. A. Marmisollé, C. Von Bilderling, E. Maza, L. Pietrasanta, F. Battaglini, M. Ceolín, O. Azzaroni, *Soft Matter* **2018**, *14*, 1939–1952.

[28] Z. Gu, T. T. Dang, M. Ma, B. C. Tang, H. Cheng, S. Jiang, Y. Dong, Y. Zhang, D. G. Anderson, *ACS Nano* **2013**, *7*, 6758–6766.

[29] X. Chen, W. Wu, Z. Guo, J. Xin, J. Li, *Biomaterials* **2011**, *32*, 1759–1766.

[30] Z. W. Lim, Y. Ping, A. Miserez, *Bioconjug. Chem.* **2018**, *29*, 2176–2180.

[31] L. Zhao, C. Xiao, L. Wang, G. Gai, J. Ding, *Chem. Commun.* **2016**, *52*, 7633–7652.

[32] K. Ariga, Q. Ji, T. Mori, M. Naito, Y. Yamauchi, H. Abe, J. P. Hill, *Chem. Soc. Rev.* **2013**, *42*, 6322.

[33] J. Shi, Z. Jiang, *J. Mater. Chem. B* **2014**, *2*, 4435.

[34] D. M. Eckmann, R. J. Composto, A. Tsourkas, V. R. Muzykantov, *J. Mater. Chem. B* **2014**, *2*, 8085–8097.

[35] Z. Zeng, Y. She, Z. Peng, J. Wei, X. He, *RSC Adv.* **2016**, *6*, 8032–8042.

[36] J. Mosquera, I. García, L. M. Liz-Marzán, *Acc. Chem. Res.* **2018**, *51*, 2305–2313.

[37] W. Tai, R. Mo, J. Di, V. Subramanian, X. Gu, J. B. Buse, Z. Gu, *Biomacromolecules* **2014**, *15*, 3495–3502.

[38] J. Yu, C. Qian, Y. Zhang, Z. Cui, Y. Zhu, Q. Shen, F. S. Ligler, J. B. Buse, Z. Gu, *Nano Lett.* **2017**, *17*, 733–739.

[39] X. Hu, J. Yu, C. Qian, Y. Lu, A. R. Kahkoska, Z. Xie, X. Jing, J. B. Buse, Z. Gu, *ACS Nano* **2017**, *11*, 613–620.

[40] Y. Zhang, J. Wang, J. Yu, D. Wen, A. R. Kahkoska, Y. Lu, X. Zhang, J. B. Buse, Z. Gu, *Small* **2018**, *14*, 1704181.

[41] Z. Tong, J. Zhou, J. Zhong, Q. Tang, Z. Lei, H. Luo, P. Ma, X. Liu, *ACS Appl. Mater. Interfaces* **2018**, *10*, 20014–20024.

[42] C. Li, X. Liu, Y. Liu, F. Huang, G. Wu, Y. Liu, Z. Zhang, Y. Ding, J. Lv, R. Ma, et al., *Nanoscale* **2019**, *11*, 9163–9175.

[43] H. G. Bagaria, M. S. Wong, *J. Mater. Chem.* **2011**, *21*, 9454–9466.

[44] Y. Lapitsky, *Curr. Opin. Colloid Interface Sci.* **2014**, *19*, 122–130.

[45] V. S. Murthy, R. K. Rana, M. S. Wong, *J. Phys. Chem. B* **2006**, *110*, 25619–25627.

[46] R. K. Rana, V. S. Murthy, J. Yu, M. S. Wong, *Adv. Mater.* **2005**, *17*, 1145–1150.

[47] B. Hu, C. Pan, Y. Sun, Z. Hou, H. Ye, B. Hu, X. Zeng, *J. Agric. Food Chem.* **2008**, *56*, 7451–7458.

[48] S. E. Plush, M. Woods, Y.-F. Zhou, S. B. Kadali, M. S. Wong, A. D. Sherry, *J. Am. Chem. Soc.* **2009**, *131*, 15918–15923.

[49] K.-I. Jang, H. G. Lee, *J. Agric. Food Chem.* **2008**, *56*, 1936–1941.

[50] N. Zhao, H. G. Bagaria, M. S. Wong, Y. Zu, *J. Nanobiotechnology* **2011**, *9*, 2.

[51] A. Farashishiko, S. E. Plush, K. B. Maier, A. Dean Sherry, M. Woods, *Chem. Commun.* **2017**, *53*, 6355–6358.

[52] V. S. Murthy, M. S. Wong, **2008**, pp. 214–232.

[53] H. Zhang, S. Mardyani, W. C. W. Chan, E. Kumacheva, *Biomacromolecules* **2006**, *7*, 1568–1572.

[54] P. G. Lawrence, Y. Lapitsky, *Langmuir* **2015**, *31*, 1564–1574.

[55] W. A. Marmisollé, J. Irigoyen, D. Gregurec, S. Moya, O. Azzaroni, *Adv. Funct. Mater.* **2015**, *25*, 4144–4152.

[56] M. L. Agazzi, S. E. Herrera, M. L. Cortez, W. A. Marmisollé, C. von Bilderling, L. I. Pietrasanta, O. Azzaroni, *Soft Matter* **2019**, *15*, 1640–1650.

[57] K. Lutz, C. Gröger, M. Sumper, E. Brunner, *Phys. Chem. Chem. Phys.* **2005**, *7*, 2812–2815.

[58] L. D'Agostino, M. Di Pietro, A. Di Luccia, *FEBS J.* **2005**, *272*, 3777–3787.

[59] J. Yu, M. A. Yaseen, B. Anvari, M. S. Wong, *Chem. Mater.* **2007**, *19*, 1277–1284.

[60] J. Yu, D. Javier, M. A. Yaseen, N. Nitin, R. Richards-Kortum, B. Anvari, M. S. Wong, *J. Am. Chem. Soc.* **2010**, *132*, 1929–1938.

[61] M. Mouslmani, J. M. Rosenholm, N. Prabhakar, M. Peurla, E. Baydoun, D. Patra, *RSC Adv.* **2015**, *5*, 18740–18750.

[62] P. Andreozzi, E. Diamanti, K. R. Py-Daniel, P. R. Cáceres-Vélez, C. Martinelli, N. Politakos, A. Escobar, M. Muzi-Falconi, R. Azevedo, S. E. Moya, *ACS Appl. Mater. Interfaces* **2017**, *9*, 38242–38254.

[63] S. E. Herrera, M. L. Agazzi, M. L. Cortez, W. A. Marmisollé, M. Tagliazucchi, O. Azzaroni, *ChemPhysChem* **2019**, *20*, 1044–1053.

[64] S. E. Herrera, M. L. Agazzi, M. L. Cortez, W. A. Marmisollé, C. Bilderling, O. Azzaroni, *Macromol. Chem. Phys.* **2019**, 1900094.

[65] K. Yoshida, R. Hashide, T. Ishii, S. Takahashi, K. Sato, J. Anzai, *Colloids Surfaces B Biointerfaces* **2012**, *91*, 274–279.

[66] W. Qi, X. Yan, J. Fei, A. Wang, Y. Cui, J. Li, *Biomaterials* **2009**, *30*, 2799–2806.

[67] K. Garajová, M. Zimmermann, M. Petrenčáková, L. Dzurová, M. Nemergut, Ľ. Škultéty, G. Žoldák, E. Sedlák, *Biophys. Chem.* **2017**, *230*, 74–83.

[68] M. D. Gouda, S. A. Singh, A. G. A. Rao, M. S. Thakur, N. G. Karanth, *J. Biol. Chem.* **2003**, *278*, 24324–24333.

[69] S. Khatun Haq, M. Faiz Ahmad, R. Hasan Khan, *Biochem. Biophys. Res. Commun.* **2003**, *303*, 685–692.

[70] B. Sharma, S. Mandani, T. K. Sarma, *J. Mater. Chem. B* **2014**, *2*, 4072–4079.

[71] J. S. Graça, R. F. de Oliveira, M. L. de Moraes, M. Ferreira, *Bioelectrochemistry* **2014**, *96*, 37–42.

[72] P. G. Lawrence, P. S. Patil, N. D. Leipzig, Y. Lapitsky, *ACS Appl. Mater. Interfaces* **2016**, *8*, 4323–4335.

[73] C. J. Thompson, L. Tetley, W. P. Cheng, *Int. J. Pharm.* **2010**, *383*, 216–227.

[74] G. Laucirica, W. A. Marmisollé, O. Azzaroni, *Phys. Chem. Chem. Phys.* **2017**, *19*, 8612–8620.

[75] R. Wilson, A. P. F. Turner, *Biosens. Bioelectron.* **1992**, *7*, 165–185.

[76] M. A. VandenBerg, M. J. Webber, *Adv. Healthc. Mater.* **2019**, *8*, 1801466.

[77] A. Matsumoto, T. Ishii, J. Nishida, H. Matsumoto, K. Kataoka, Y. Miyahara, *Angew. Chemie Int. Ed.* **2012**, *51*, 2124–2128.

10.1002/chem.201905075

Table of Contents